Right Parietal Brain Activity Precedes Perceptual Alternation During Binocular Rivalry

Juliane Britz,[1]* Michael A. Pitts,[2] and Christoph M. Michel[2]

[1]*Department of Fundamental Neuroscience, University of Geneva, Geneva, Switzerland*
[2]*Department of Neurosciences, University of California, San Diego, California*

Abstract: We investigated perceptual reversals for intermittently presented stimuli during binocular rivalry and physical alternation while the ongoing EEG was recorded from 64 channels. EEG topographies immediately preceding stimulus-onset were analyzed and two topographies doubly dissociated perceptual reversals from non-reversals. The estimated intracranial generators associated with these topographies were stronger in right inferior parietal cortex and weaker bilaterally in the ventral stream before perceptual reversals. No such differences were found for physical alternation of the same stimuli. These results replicate and extend findings from a previous study with the Necker cube and suggest common neural mechanisms associated with perceptual reversals during binocular rivalry and ambiguous figure perception. For both types of multi-stable stimuli, the dorsal stream is more active preceding perceptual reversals. Activity in the ventral stream, however, differed for binocular rivalry compared to ambiguous figures. The results from the two studies suggest a causal role for the right inferior parietal cortex in generating perceptual reversals regardless of the type of multi-stable stimulus, while activity in the ventral stream appears to depend on the particular type of stimulus. *Hum Brain Mapp 32:1432–1442, 2011.* © 2010 Wiley-Liss, Inc.

Key words: EEG; EEG mapping; binocular rivalry; inverse solution; LORETA; right inferior parietal

INTRODUCTION

Binocular rivalry arises when two dissimilar images are presented simultaneously to the two eyes. The resulting percept is not a stable composite of the two competing images, but perceptual awareness alternates stochastically every few seconds between the two rivaling percepts. Because these perceptual alternations happen spontaneously and randomly and without any changes in the physical input, binocular rivalry and other forms of multi-stable perception such as bi-stable ambiguous figures are powerful tools for dissociating perceptual awareness from sensory processing [Sterzer et al., 2009].

Both the mechanisms and timing of perceptual dominance/suppression remain a matter of debate. The effects of binocular rivalry occur in many areas along the visual stream. For example, functional imaging studies in humans suggest that rivalry is already resolved at the earliest stages of visual processing, namely the LGN and V1 [Haynes et al., 2005; Lee et al., 2005; Polonsky et al., 2000; Wunderlich et al., 2005] and extrastriate areas [Haynes and Rees, 2005; Meng et al., 2005; Tong et al., 1998]. On the other hand, electrophysiological studies in non-human primates have failed to show the resolution of binocular rivalry at these early stages; they found that local field potentials (LFPs) in extrastriate visual areas and in inferior temporal cortex reflect the currently active percept

Contract grant sponsor: National Institutes of Health; Contract grant numbers: 5 T32 MH20002, 2 R01 EY016984-35; Contract grant sponsor: The Swiss National Science Foundation; Contract grant number: 32003B-118315; Contract grant sponsors: The Center for Biomedical Imaging (CIBM) of the Geneva and Lausanne Universities, EPFL, The Leenaards and Louis-Jeantet foundations.

*Correspondence to: Juliane Britz, Ph.D., Department of Fundamental Neuroscience, Centre Médical Universitaire, 1 Rue Michel Servet, CH-1211 Genève, Switzerland.
E-mail: juliane.britz@unige.ch

Received for publication 18 May 2010; Accepted 5 June 2010
DOI: 10.1002/hbm.21117
Published online 5 August 2010 in Wiley Online Library (wileyonlinelibrary.com).

[Leopold and Logothetis, 1996; Logothetis et al., 1996; Logothetis and Schall, 1989; Sheinberg and Logothetis, 1997]. In addition to visual areas, activity in frontal and parietal areas is also modulated as a function of subjective visual awareness [Lumer et al., 1998; Lumer and Rees, 1999]. Thus, many of the brain areas involved in binocular rivalry have been identified, but much less is known about the exact timing underlying the suppression of a percept and the emergence of its rivaling counterpart.

Recent ERP studies have begun to investigate the timing of perceptual alternations during ambiguous figure perception [Britz et al., 2009; Kornmeier and Bach, 2004, 2005, 2006; Pitts et al., 2009]. These studies identified ERP components associated with perceptual reversals of a Necker cube (or Necker lattice) during intermittent presentation, which allows precise time-locking of the EEG with stimulus onsets. These reversal-related components occurred during two time periods after stimulus onset: an occipital negativity at ~250 ms ("Reversal Negativity") and a parietal positivity at ~340 ms ("Late Positive Component"). Both of these components were also elicited by physical reversals of an unambiguous lattice [Kornmeier and Bach, 2004]. Although these ERP studies indicate rather late effects that are similar for physical and endogenous alternations, we recently demonstrated differences in electrocortical activity between reversal and non-reversal perception immediately before stimulus onset [Britz et al., 2009]. This dissociation of perceptual reversals from non-reversals was evident in the global momentary brain state reflected by the EEG topography at the time of stimulus arrival. The sources of the concomitant generators of these EEG topographies differed in the right inferior parietal lobe, suggesting a role for the parietal cortex in initiating perceptual alternations. Although binocular rivalry and ambiguous figure perception arise from different processes—namely the suppression/dominance of two monocular stimuli and the mutually exclusive interpretations of the same ambiguous stimulus—they share a common phenomenology, namely spontaneous alternations of perception despite constant sensory stimulation. It is thus possible that these internally generated alternations arise from a common process that may be reflected by common pre-stimulus brain states that cause perceptual change.

In the present study, we used Electrical Neuroimaging [Michel et al., 2009; Murray et al., 2008] to investigate spontaneous perceptual alternations in binocular rivalry using an intermittent stimulus presentation [Kornmeier and Bach, 2004]. We hypothesized that perceptual alternations in binocular rivalry are generated internally and spontaneously and that the momentary state of the brain should determine the fate of the incoming rivaling stimulus. The EEG topography, that is, the configuration of the scalp potential field is a direct measure of the momentary global state of the brain. It reflects the spatial summation of all concurrently active intracranial electrical sources irrespective of their frequency that can be measured at the surface of the scalp. Several studies have shown that the topography of the scalp potential field remains stable for short periods of time (~100 ms), presumably reflecting the momentary mind state [Lehmann et al., 1993, 2010]. We have recently shown that these different topographies (so-called microstates) correlate with some of the well-known resting states, indicating that different networks might be momentarily active when the stimulus is presented [Britz et al., 2010]. Since this activation pattern changes about every 100 ms, we assume that the momentary state just within the 100 ms around the stimulus is most crucial for determining the fate of the stimulus. Previous studies support this hypothesis [Britz et al., 2009; Kondakor et al., 1995, 1997; Lehmann et al., 1998; Mohr et al., 2005].

We contrasted internally generated perceptual reversals during binocular rivalry with physical alternations of the same stimuli when presented monocularly and according to our hypothesis, only the internally generated, but not the physically driven perceptual alternations should manifest in different EEG topographies immediately before stimulus onset. Under both conditions, we assessed the momentary topography of the pre-stimulus state and their concomitant source differences by means of distributed source localization procedures. Differences in topography necessarily imply different generators [Helmholtz, 1853; Vaughan, 1982], whereas the opposite is not necessarily true: identical topographies can be generated by different sources. Like all EEG and MEG source localization methods, the distributed inverse solutions are non-unique and depend on the implemented constraints and regularization parameters of the source model. However, numerous studies provide compelling evidence that distributed linear inverse solutions provide reasonable source estimates [Groening et al., 2009; James et al., 2009; Laganaro et al., in press; Michel et al., 2004; Murray et al., 2006; Schulz et al., 2008; Vulliemoz et al., 2009; Zumsteg et al., 2006].

On the basis of previous findings for the Necker cube [Britz et al., 2009], we further hypothesized that spontaneous perceptual reversals for binocular rivalry would manifest in increased activity in right inferior parietal cortex. Because this reversal-related activity is assumed to be internally generated, we also predicted no such effects for the physical alternation of the same stimuli.

METHODS

Subjects

Fourteen healthy adults (8 female, mean age 20 years, range 18–23) participated in the two experiments (binocular rivalry and physical alternation) on separate days; the order of experiments was counterbalanced across subjects. One subject was excluded from the analyses due to substantial contamination by artifacts, and the data of 13 subjects were submitted to subsequent analyses. All had normal or corrected-to normal visual acuity and no history of psychiatric or neurological impairments. All participants were recruited as volunteers and gave informed

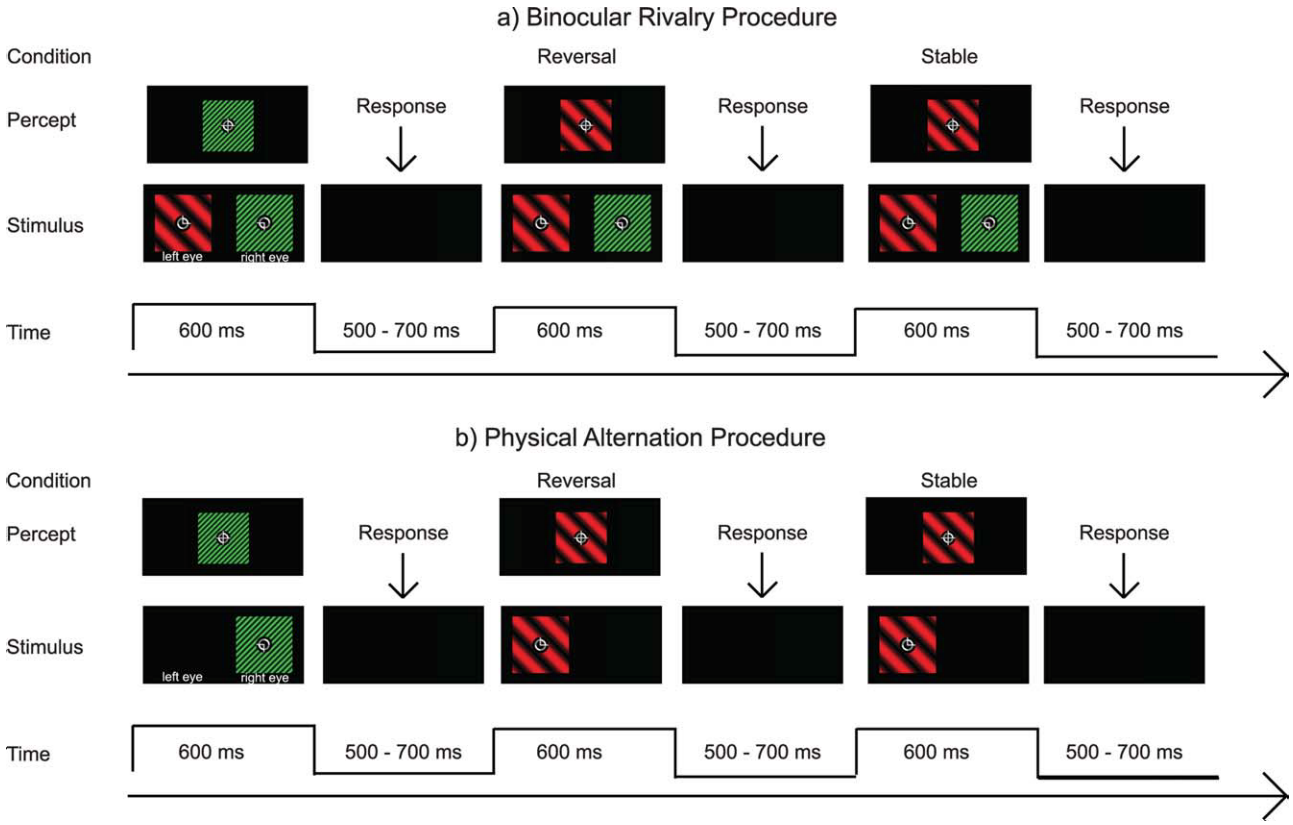

Figure 1.

Stimuli and task. (**a**) Binocular rivalry procedure. Subjects viewed monocular pairs of Gabor gratings orthogonal in color, orientation, and spatial frequency and indicated the color of their percepts via button-presses. (**b**) Physical alternation procedure. Subjects viewed successions of one stimulus of a pair while again reporting the color of their percepts. [Color figure can be viewed in the online issue, which is available at wileyonlinelibrary.com.]

consent prior to each experiment. The experimental procedures were approved by the University of California at San Diego Institutional Review Board.

Stimuli and Procedure

We first titrated the optimal durations for both the stimulus presentation and the blank intervals in a behavioral pilot study such that in each trial, only one of the rivaling images could be clearly perceived and that no reversals occurred during the presentation. This was based in part on evidence from behavioral studies showing that dichoptic orthogonal gratings fuse into "plaids" when presented for less than 150 ms [Wolfe, 1983] on the one hand and that the extension of the inter-stimulus interval to several seconds prevents perceptual reversals altogether [Leopold et al., 2002; Sterzer and Rees, 2008].

Stimuli were presented on a black background and centered horizontally within the left and right halves of a CRT computer screen with a refresh rate of 60 Hz. Subjects viewed the stimuli through a mirror-stereoscope which allows the separate stimulation of the left and right eyes. Participants adjusted the angle of the mirrors to achieve stereo fusion. To help maintain fusion, a fixation cross (1°) was presented in the center of a gray/white circle (0.75°). All stimuli were presented at fixation. Figure 1 illustrates the stimuli and experimental procedure.

In the binocular rivalry experiment, stimuli were presented as pairs, one to each eye. They were square-shaped sinusoidal gratings subtending 6° of visual angle in diameter. To minimize piece-meal rivalry, the pairs were orthogonal on three dimensions: color (red vs. green), orientation (45° vs. 135°), and spatial frequency (1 cpd vs. 5 cpd). Including the factor eye (left vs. right), this yielded eight different pairs of stimuli. Each pair was equated in luminance (by chromatic photometry) and was presented in six non-consecutive blocks of trials (counterbalanced across blocks), yielding 48 blocks. During each block, stimuli were presented 50 times (~1 min), and subjects took self-paced breaks between blocks. All stimuli were presented intermittently for 600 ms, and the inter-stimulus interval varied randomly between 500 and 700 ms.

For each stimulus, participants were asked to indicate the color of their percept by means of a button press. They were instructed to withhold their response in the case that they perceived a piece-meal mixture between the two stimuli.

In the physical alternation experiment, only one stimulus of a pair was presented to one eye, and the input to the other eye was kept blank. The two stimuli of a pair were presented in alternation at rates that mimicked the switching rates under binocular rivalry with random alternations every 1.2–6.0 s. To equate the response-task between the rivalry and physical alternation conditions, subjects were again asked to indicate the color of their percept after each stimulus presentation.

EEG Acquisition and Raw Data Processing

The EEG was recorded from 64 tin electrodes mounted in an elastic cap (Electrocap International), band-pass filtered between 0.1 and 80 Hz continuously digitized at 250 Hz and amplified with a battery-powered amplifier (SA Instrumentation) with a gain of 10,000. Impedances were kept below 5 kΩ, and the EEG was referenced online to the right mastoid. Horizontal and vertical eye movements were monitored with a bilateral external canthus montage and a sub-orbital electrode referenced to the right mastoid; offline the EEG was re-computed to the common average reference.

The analysis was performed using the Cartool software by Denis Brunet (http://brainmapping.unige.ch/Cartool.htm). Before selecting the relevant EEG epochs, we first removed the DC component and then band-pass filtered the raw EEG between 1 and 30 Hz. A 2nd order Butterworth filter with a −12 db/octave roll-off was used. The filter was computed linearly with two passes (one forward and one backward), eliminating the phase shift, and with poles calculated each time to the desired cut-off frequency. This was done using epochs spanning −500 to +500 ms around the selected epoch.

For each stimulus, we determined whether perception alternated (reversed) or remained the same (stable) by comparing the current response with the response to the preceding stimulus. The EEG was then segmented into epochs ranging from 50 ms before until stimulus onset. Epochs contaminated by oculomotor and other artifacts were rejected.

Analysis of Behavioral Data and Statistical Properties of the Reversal Intervals

We computed the average and median durations for the reversal intervals and the reaction times. We then assessed the statistical properties of the reversal intervals by means of their autocorrelation function and by means of their distribution. The reversal intervals of binocular rivalry do not show short-term intercorrelations [Lehky, 1995; Mamassian and Goutcher, 2005] and can be approximated by gamma [Leopold and Logothetis, 1999] and lognormal [Lehky, 1995] functions.

We evaluated the autocorrelation function of the reversal intervals by correlating the reversal duration in trial n with that in trial $n + m$ with $m = 1{:}10$. We assessed the distribution of these durations by computing the Maximum Likelihood Estimates of the parameters from the cumulative probability distribution both of the scale and shape parameters (α and β) of the gamma distribution and mean and standard deviation (μ and σ) of the lognormal distribution. We used a Kolmogorov-Smirnov test to assess these distributions.

We further evaluated whether the stable and reversal trials differed systematically with respect to piece-meal percepts in the preceding trial.

Analysis of Pre-Stimulus Global EEG States

The momentary scalp topography of the EEG reflects all concurrently active sources of the brain irrespective of their frequency [Lehmann et al., 1987]. The topography of the scalp potential field remains quasi-stable for short periods (~80–120 ms) during which only its strength, but not its configuration vary [Koenig et al., 2002; Lehmann et al., 2009]. These periods of stability have been termed "functional microstates" [Lehmann and Skrandies, 1980] which have been found to influence both perception [Britz et al., 2009] and cognition [Mohr et al., 2005] and to characterize the nature of spontaneous thoughts [Lehmann et al., 1998]. The latter of these studies found that the behavioral response could only be related to the microstate immediately prior to the stimulus onset (in that case, an auditory prompt), which is why subsequent studies focused only on the microstate immediately before stimulus onset. A measure of field strength is the global field power (GFP), which is equivalent to the spatial standard deviation of the potential field [Lehmann and Skrandies, 1980], and consequently, the maximum of the GFP is the best representative of a momentary microstate in terms of signal-to-noise-ratio. As the average duration of a microstate is about 100 ms and the arrival of a stimulus does not "disrupt" a momentary microstate, we reasoned that the GFP maximum in the 50 ms before the onset is the best representative of the microstate immediately before the stimulus onset. We thus extracted the map representing the momentary scalp topography of the GFP maximum in the 50 ms before stimulus onset that was temporally closest to the stimulus onset as the representative of the pre-stimulus microstate in each trial [Britz et al., 2009; Kondakor et al., 1995, 1997; Lehmann et al., 1994; Mohr et al., 2005].

We used a spatial cluster analysis to identify the most dominant EEG microstates [Michel et al., 2004; Pascual-Marqui et al., 1995]. An Atomize-Agglomerate Hierarchical Clustering (AAHC) method was used [Britz et al., 2009; Murray et al., 2008]. The cluster analysis yields templates of the most dominant topographies that represent the microstates. The optimal number of clusters, that is, the best solution of the cluster analysis was determined by

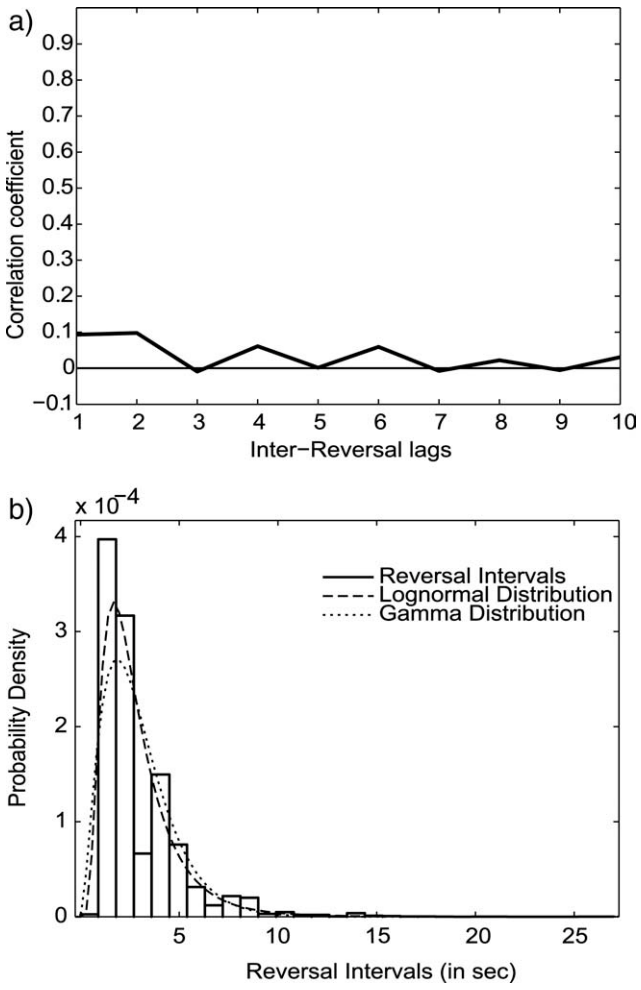

Figure 2.

Statistical properties of the reversal intervals. (**a**) Autocorrelation function of the reversal intervals for the lags 1–10. The *y*-axis shows the correlation coefficients for the respective lags. (**b**) Histogram and probability density function of the reversal intervals. The dashed line represents the fitted lognormal function and the dotted line the fitted gamma function.

means of the cross-validation criterion [Pascual-Marqui et al., 1995]. The cross-validation criterion is a measure of predictive residual variance. The minimum of the cross validation criterion is considered as the optimal number of clusters, that is, the number of clusters for which the residual variance is minimal. The template maps of these clusters correspond to the mean of all maps belonging to this cluster. We made no a priori assumptions on the number of clusters or on the minimum of explained variance, because we wanted our analysis to be strictly data driven.

In a first step, we identified those maps, that is, the scalp topography representing the momentary microstate, that best differentiate the Reversal and Stable conditions *within* each subject. We then computed a spatial correlation between the template maps and all extracted maps and matched (i.e., labeled) each GFP peak with the template map it best corresponded with. On the basis of measures of frequency of occurrence and global explained variance, we determined the two maps that best differentiated the Reversal and Stable conditions within each subject.

In a second step, we identified those maps that best differentiate the Reversal and Stable conditions *across* subjects. We concurrently submitted all those maps identified in the first step to a second AAHC cluster analysis and determined its best solution by means of the cross-validation criterion. We then computed the spatial correlation between the templates of the best solution and all maps submitted to the 2nd cluster analysis. We finally determined which maps best differentiated the Reversal and Stable conditions across subjects by statistically comparing their frequency of occurrence and global explained variance between the two conditions.

Analysis of Pre-Stimulus Source Differences

We extracted the maps that best differentiated the Reversal and Stable condition across subjects (i.e., that were identified in the 2nd cluster analysis) from each individual and estimated their intracranial current distributions with a LORETA inverse solution. LORETA was calculated in a simplified realistic head model called SMAC [Spinelli et al., 2000]: The average template brain of the Montreal Neurological Institute (MNI) was used as standard brain for all subjects. The brain surface was extracted from this MRI and the best fitting sphere was estimated. Then the MRI was warped according to the ratio of the sphere radius and the real surface radius. Three thousand five solution points were then defined in regular distances within the gray matter of this standard brain. The forward problem was then solved with an analytical solution with a 3-layer conductor model. Additional details can be found in Michel et al. [2004]. The simplified realistic head model offers an easy and fast extraction of the head model and a fast and accurate analytical solution to the forward problem at the expense of being maybe somewhat less precise than finite element models based on the individual anatomy. Nevertheless, accurate source localization using this head model has been demonstrated in different clinical and experimental studies in the past [Groening et al., 2009; Michel et al., 2004; Phillips et al., 2005; Sperli et al., 2006; Vulliemoz et al., 2009].

We used conservative statistical analyses to investigate differences between the source estimations of the two conditions, which helps to eliminate spurious sources of activity. Equivalent to statistical parametric mapping in fMRI, we assessed their statistical difference by means of paired *t* tests between the Reversal and Stable conditions at each solution points. The *P* values were adjusted for multiple testing with the Sidak correction [Sidak, 1967]. We used the number of electrodes ($n = 63$) as the independent measure because in EEG source imaging the electrodes on the scalp constitute the independent measures, not the solution points [Grave de Peralta Menendez et al., 2004; Michel et al., 2004].

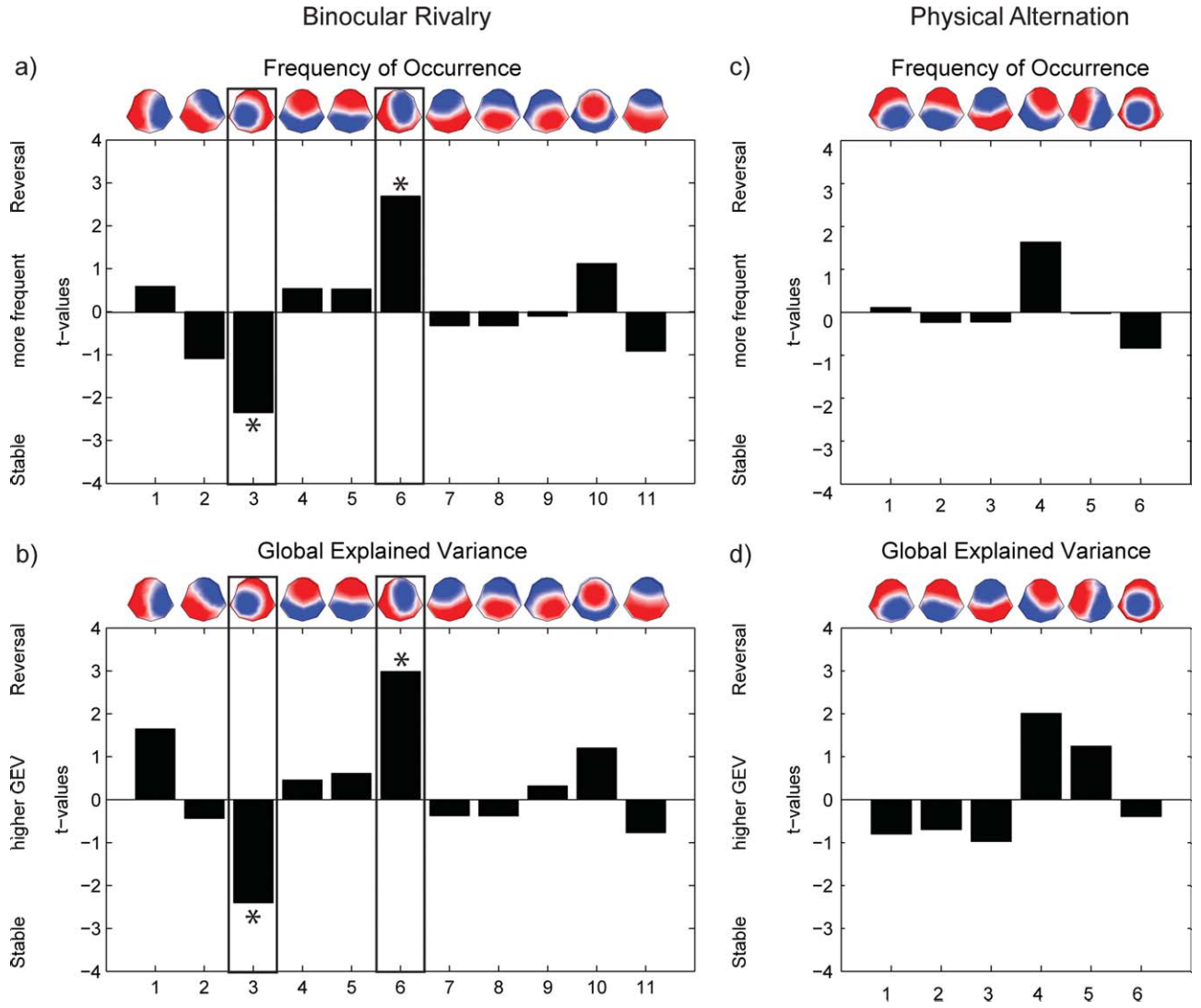

Figure 3.

Templates of the pre-stimulus microstates identified by the cluster analysis. The two maps that doubly dissociated the two conditions are labeled. (**a**) The *t* values for the statistical comparison of the Frequency of Occurrence in the Reversal and Stable condition for each map in the rivalry experiment. The asterisk indicates statistically significant differences. (**b**) The *t* values for the statistical comparison of the Global Explained Variance in the Reversal and Stable condition for each map in the rivalry experiment. The asterisk indicates statistically significant differences. (**c**) The *t* values for the statistical comparison of the Frequency of Occurrence in the Reversal and Stable condition for each map in the physical alternation experiment. (**d**) The *t* values for the statistical comparison of the Global Explained Variance in the Reversal and Stable condition in the physical alternation experiment. [Color figure can be viewed in the online issue, which is available at wileyonlinelibrary.com.]

RESULTS

Behavioral Results and Statistical Properties of the Reversal Intervals

After artifact rejection, an average of 1,030 reversal and 1,238 stable trials were obtained for each subject, yielding a total of 13,394 reversal and 16,095 stable trials. The reversal intervals had a mean and median duration of 3,052 and 2,448 ms, respectively, and a standard deviation of 2,080 ms. The mean reaction time was 529 ms, and reactions were performed on average 609 ms before the onset of the next stimulus. The autocorrelation function of the reversal intervals (Fig. 2a) shows that there were no correlations between the reversal intervals in a trial *n* and those of the subsequent 10 reversals. Figure 2b,c show the Probability Density Function and Cumulative Probability

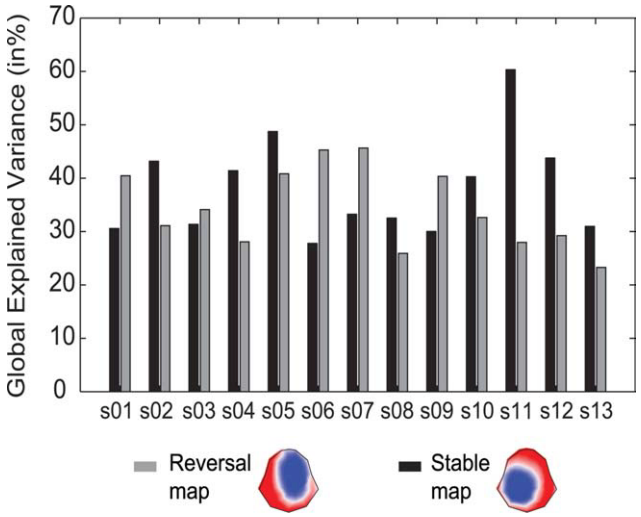

Figure 4.

Global presence of the template maps. Bars indicate the percentage of Global Explained Variance of the Reversal (light gray) and Stable (dark gray) map in each individual subject. [Color figure can be viewed in the online issue, which is available at wileyonlinelibrary.com.]

Function, respectively. A Kolmogorov-Smirnov test revealed that the reversal intervals followed both a gamma ($\alpha = 2.73$, $\beta = 1.065$, $P = 0$) and a lognormal ($\mu = 2917.68$, $\sigma = 2086.01$, $P = 0$) distribution.

In the Stable condition, 1.3% (±1.7%) of trials were preceded by piece-meal percepts, and in the Reversal condition, 1.8% (1.8%) of trials were preceded by piece-meal percepts. This difference was not significant ($t < 1$).

Pre-Stimulus EEG Microstates

Binocular rivalry experiment

In the first step, we identified those maps that best differentiate the Reversal and Stable conditions within each subject. The cross-validation criterion in the AAHC cluster analysis identified on average 6.3 (±1.6) template maps as the optimal solution which explained on average 68.02% (±7.24%) of the Global Variance. We computed a strength-independent spatial correlation between the templates and all maps and thus identified the two maps that best differentiated the Reversal and Stable conditions in each subject based on their frequency of occurrence, that is, we retained the one map that occurred most frequently in the Reversal and the one that occurred most frequently in the Stable condition.

In the second step, we determined which maps best differentiate the Reversal and Stable conditions across subjects. We retained the maps identified in the first step and submitted them to a 2nd AAHC cluster analysis. The cross validation criterion identified 11 maps as the optimal solution (Fig. 3a,b). These 11 maps explained 75.29% of the variance. We computed again a strength-independent spatial correlation between the 11 templates and all maps and statistically compared their frequency of occurrence. Two maps doubly dissociated the Reversal and Stable conditions both in terms of Frequency of Occurrence and Global Explained Variance (Reversal: Frequency of Occurrence: $t = 2.35$, $P = 0.047$, GEV: $t = 2.4$, $P = 0.034$; Stable: Frequency of Occurrence: $t = 2.69$, $P = 0.012$, GEV: $t = 2.98$, $P = 0.012$). To make sure that these maps could be identified in all subjects, we determined their global presence by means of the variance they explained in each subject (Fig. 4). Both maps could be identified in each subject, and they explained 38% and 34.21% of the variance.

Physical alternation experiment

In the first step, we again identified those maps that best differentiate the Reversal and Stable conditions within each subject. The AAHC cluster analysis identified on average 6.69 (±1.03) template maps as the optimal solution which explained on average 69.23% (±7.05%) of the Global Variance. Again, we identified those two maps that differentiated the Reversal and Stable conditions in each subject based on their frequency of occurrence.

In the 2nd step, we determined which maps differentiate the two conditions across subjects. We retained the maps determined in the first step and submitted them to a 2nd AAHC cluster analysis. The cross validation criterion identified six maps as the optimal solution. These six maps explained 67.45% of the variance (Fig. 3c,d). We computed again a strength-independent spatial correlation between the six templates and all maps and statistically compared their frequency of occurrence. We did not identify any map that could significantly dissociate the two conditions.

Pre-Stimulus Source Differences

Binocular rivalry experiment

We computed distributed LORETA inverse solutions for the two pre-stimulus EEG maps that doubly dissociated the Reversal and Stable conditions and compared the statistical differences of their intracranial generators across subjects by paired t tests at each solution point (Fig. 5). Positive differences, that is, increased activations before Reversals were found in the Right Inferior Parietal Lobule (Talairach coordinates of the maximum: 50 −50 45, $t = 3.95$, $P = 0.006$). Negative differences, that is, decreased activations before Reversals were found bilaterally in the ventral stream the Middle Occipital Gyrus (left: −43 −74 −3, $t = -3.02$, $P = 0.02$; right: 43 −68 −8; $t = 4.37$, $P = 0.004$), left Fusiform Gyrus (−42 −45 −13, $t = -3.73$, $P = 0.008$); and the Middle and Inferior Temporal Gyri. Activation foci are summarized in Table I.

DISCUSSION

We investigated pre-stimulus brain states associated with perceptual reversals during binocular rivalry by

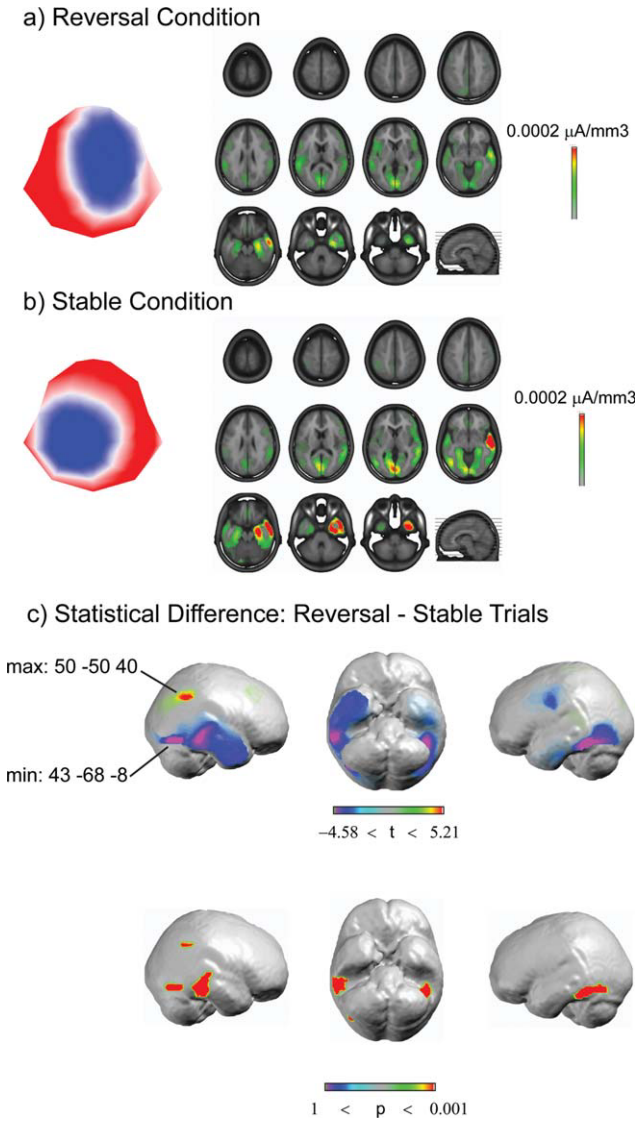

Figure 5.

Pre-stimulus map sources and source differences. (**a**) LORETA source estimation for the Reversal template map. (**b**) LORETA source estimation for Stable template map. (**c**) Statistical parametric maps (*P* values on the top and *t* values on the bottom) depicting significant differences for the LORETA source estimations depicted in a and b. Orange–red colors indicate stronger current densities in the Reversal condition and blue–violet colors indicate stronger differences in the Stable condition.

using an intermittent stimulus presentation approach. Two pre-stimulus EEG topographies that doubly dissociate perceptual reversals from non-reversals were identified. Statistical parametric mapping of their estimated intracranial current densities revealed increased current density in the right inferior parietal lobe and decreased current density in bilateral lateral occipital and temporal areas preceding perceptual reversals These findings replicate and extend our previous findings for reversals of the Necker cube [Britz et al., 2009], in which we likewise identified two pre-stimulus scalp topographies that doubly dissociated perceptual reversals from perceptual stability. Also, the concomitant intracranial generators differed in virtually the same area in the right inferior parietal lobe preceding reversals of the Necker cube and reversals during rivalry. As temporal precedence provides evidence for a putative causal role, these results provide strong evidence for the idea that this area plays a central role in the initiation of perceptual reversals irrespective of whether the reversals are between different perceptual interpretations of an ambiguous figure or between competing monocular stimuli. This finding sheds new light on the differential role of top–down influence in ambiguous figure perception and binocular rivalry. Previous research suggests that binocular rivalry is less susceptible to top–down modulation than ambiguous figure perception [Meng and Tong, 2004]: subjects can more easily control their perception of ambiguous figures than of binocularly rivaling stimuli when instructed to do so. We did not manipulate volitional control over perceptual reversals in our two studies, so our results are not directly comparable to those of Meng and Tong. What we can state from the results in the present and our previous study is that the spontaneous reversals of both ambiguous figures and during binocular rivalry recruit the same higher level and non-visual brain areas immediately preceding reversals. The temporal order of activity suggests that those higher level areas become active before primary sensory areas which could be interpreted as top–down influence. The right inferior parietal lobe has been consistently identified in fMRI studies using bi-stable ambiguous stimuli [Inui et al., 2000; Kleinschmidt et al., 1998; Slotnick and Yantis, 2005] and binocular rivalry [Lumer et al., 1998; Lumer and Rees, 1999; Wilcke et al., 2009], but its function had been interpreted as an appraisal of the altered percept rather than its cause. This area has been found to be involved in change detection and change blindness [Beck et al., 2001, 2006; Kim and Blake, 2005; Pessoa and Ungerleider, 2004]. Other studies have found that this same area is important for reorienting attention [Corbetta, 1998; Corbetta et al., 2000, 2008]. It appears that activity in this area biases an altered perception of the incoming stimulus, possibly by reorienting attention. Because of the slow time-course of the hemodynamic response function, the temporal and functional implications of fMRI activations remain a challenge. With the precise temporal resolution of Electrical Neuroimaging, we found that this region was activated immediately prior to reversals, which suggests that its role may be causal. Further evidence for a causal role of right inferior parietal cortex for perceptual reversals comes from a study in which repetitive Transcranial Magnetic Stimulation (rTMS) over right, but not left, inferior parietal cortex decreased perceptual reversals of the continuous wagon wheel

TABLE I. Foci of statistical differences in current density of the pre-stimulus EEG maps in the reversal and stable conditions

	x	*y*	*z*	*t*	*P*
Positive difference					
Right Inferior Parietal Lobe	50	−50	45	3.95	0.006
Negative differences					
Left Middle Occipital Gyrus	−43	−74	3	−3.025	0.02
Right Middle Occipital Gyrus	43	−68	−8	−4.38	0.004
Left Fusiform Gyrus	−42	−45	−13	−3.73	0.008
Left Middle Temporal Gyrus	−74	−55	1	−2.88	0.024
Right Middle Temporal Gyrus	43	−68	−8	−4.38	0.004
Left Inferior Temporal Gyrus	−48	−50	−13	−3.54	0.001
Right Inferior Temporal Gyrus	45	−6	−31	−2.944	0.022

illusion [VanRullen et al., 2008]. Also, our current findings confirmed that this right parietal activation is associated with endogenously driven but not exogenously driven perceptual switches. We found no differences in pre-stimulus scalp topography for the physical alternation of the same stimuli.

The role of non-sensory brain areas in the initiation of perceptual alternations has been described in both lesion and fMRI studies [Sterzer and Kleinschmidt, 2007; Windmann et al., 2006]. They suggest a role of bilateral prefrontal areas in the control over multi-stable perception. Patients with pre-frontal lesions show normal spontaneous reversal rates for ambiguous figures, but they can not voluntarily generate perceptual reversals [Windmann et al., 2006]. Likewise, the temporal precedence of activity in non-visual areas (right inferior frontal cortex) over that in visual areas suggests a causal role of the former in initiating perceptual reversals [Sterzer and Kleinschmidt, 2007]. In a previous study using an intermittent presentation of an ambiguous figure [Britz et al., 2009] we found bilateral prefrontal activity in the retention interval preceding both reversal and stable trials, however, it was not modulated differently for perceptual reversals. In the present study, we found no specific activation of the prefrontal cortex in the time period immediately preceding perceptual reversals.

The present finding also extends the findings from our previous study. In addition to increased parietal activity preceding reversals, we found increased activity in bilateral lateral occipital and inferior temporal areas preceding non-reversals. Single-cell recordings from awake behaving monkeys showed that discharge rates in extrastriate visual and inferior temporal areas reflect the reported percept during continuous stimulus presentation [Leopold and Logothetis, 1996; Logothetis and Schall, 1989; Sheinberg and Logothetis, 1997].

To our knowledge, this is the first EEG study that has used an intermittent instead of a continuous stimulus presentation during binocular rivalry and has focused on perceptual reversals vs. non-reversals. One could argue that this intermittent presentation might not yield "natural" reversal conditions. However, the intermittent presentation of bi-stable ambiguous stimuli elicits reversal rates similar to continuous stimulus presentation [Britz et al., 2009; Kornmeier et al., 2007]. Our analyses of the statistical properties of the reversal intervals, namely their autocorrelation function and their distribution show that our subjects showed the same behavior as under continuous stimulus presentation: the reversal intervals have virtually the same duration, they occur randomly, i.e. without a clear periodicity and they follow a gamma and lognormal function.

Eye movements—or rather retinal image shifts—have been shown to cause perceptual alternations during binocular rivalry during continuous stimulus presentation: saccades occurred ~500–100 ms prior to button presses indicating perceptual reversals [van Dam and van Ee, 2006]. However, to our knowledge, eye movements have never been shown to induce perceptual reversals during an intermittent stimulus presentation. We did not monitor eye movements in our study, so we can not completely rule out that they induced the perceptual reversals, but we are rather sure that our intermittent stimulus presentation precluded saccades as the cause of perceptual reversals. Given the timing between saccades and button presses on one hand and the timing of our intermittently presented stimuli on the other hand, saccades that might have occurred while the stimuli were on the screen—which lead to retinal image shifts—would have caused perceptual reversals in the time window when the screen was blank. Saccades during the blank interval—which leave the retinal image unaltered—could not have caused perceptual reversals.

An alternative explanation of our pre-stimulus findings might be that they represent post-response effects rather than pre-reversal effects. However, this explanation is rather unlikely because subjects reported their percept in every trial, such that every stimulus is both followed and preceded by a motor response. Moreover, reactions were performed on average 609 ms before each stimulus, that is, well before the time window we analyzed.

Conclusions

Although perceptual alternations elicited during binocular rivalry and bi-stable ambiguous figures may seem to arise from fundamentally different processes, that is, mutually exclusive interpretations of an ambiguous stimulus versus suppression/dominance of one of two monocular images, the current study suggests that the neural events preceding perceptual reversals may be similar. Both types of reversals occur randomly and are generated internally, and both can be related to the momentary state of the brain at the moment of stimulus arrival. For both the Necker cube and binocular rivalry increased activity in the right inferior parietal lobe precedes perceptual reversals which supports the notion that it is causal for the

generation of these reversals. No such common mechanism was identified when the percept remains stable; perceptual stability appears to depend on the kind of stimuli, whereas perceptual reversals are generated by the same mechanism irrespective of the physical nature of the stimuli.

ACKNOWLEDGMENTS

The Cartool software (http://brainmapping.unige.ch/Cartool.htm) has been programed by Denis Brunet from the Functional Brain Mapping Laboratory, Geneva, Switzerland.

REFERENCES

Beck DM, Rees G, Frith CD, Lavie N (2001): Neural correlates of change detection and change blindness. Nat Neurosci 4: 645–650.

Beck DM, Muggleton N, Walsh V, Lavie N (2006): Right parietal cortex plays a critical role in change blindness. Cereb Cortex 16:712–717.

Britz J, Landis T, Michel CM (2009): Right parietal brain activity precedes perceptual alternation of bistable stimuli. Cereb Cortex 19:55–65.

Britz J, Van De Ville D, Michel CM: BOLD correlates of EEG topography reveal rapid resting-state network dynamics. Neuroimage 52:1162–1170.

Corbetta M (1998): Frontoparietal cortical networks for directing attention and the eye to visual locations: Identical, independent, or overlapping neural systems? Proc Natl Acad Sci USA 95:831–838.

Corbetta M, Kincade JM, Ollinger JM, McAvoy MP, Shulman GL (2000): Voluntary orienting is dissociated from target detection in human posterior parietal cortex. Nat Neurosci 3:292–297.

Corbetta M, Patel G, Shulman GL (2008): The reorienting system of the human brain: From environment to theory of mind. Neuron 58:306–324.

Grave de Peralta Menendez R, Murray MM, Michel CM, Martuzzi R, Gonzalez Andino SL (2004): Electrical neuroimaging based on biophysical constraints. Neuroimage 21:527–539.

Groening K, Brodbeck V, Moeller F, Wolff S, van Baalen A, Michel CM, Jansen O, Boor R, Wiegand G, Stephani U (2009): Combination of EEG-fMRI and EEG source analysis improves interpretation of spike-associated activation networks in paediatric pharmacoresistant focal epilepsies. Neuroimage 46:827–833.

Haynes J-D, Rees G (2005): Predicting the stream of consciousness from activity in human visual cortex. Curr Biol 15:1301–1307.

Haynes JD, Deichmann R, Rees G (2005): Eye-specific effects of binocular rivalry in the human lateral geniculate nucleus. Nature 438:496–499.

Helmholtz HLF (1853): Über einige Gesetze der Vertheilung elektrischer Ströme in körperlichen Leitern mit Anwendung auf die thierisch-elektrischen Versuche. Annalen der Physik und Chemie 9:221–233.

Inui T, Tanaka S, Okada T, Nishizawa S, Katayama M, Konishi J (2000): Neural substrates for depth perception of the Necker cube: A functional magnetic resonance imaging study in human subjects. Neurosci Lett 282:145–148.

James C, Morand S, Barcellona-Lehmann S, Michel CM, Schnider A (2009): Neural transition from short- to long-term memory and the medial temporal lobe: A human evoked-potential study. Hippocampus 19:371–378.

Kim C-Y, Blake R (2005): Psychophysical magic: Rendering the visible invisible. Trends Cogn Sci 9:381–388.

Kleinschmidt A, Büchel C, Zeki S, Frackowiak RS (1998): Human brain activity during spontaneously reversing perception of ambiguous figures. Proc R Soc Lond Ser B: Biol Sci 265:2427–2427.

Koenig T, Prichep L, Lehmann D, Sosa PV, Braeker E, Kleinlogel H, Isenhart R, John ER (2002): Millisecond by Millisecond, Year by Year: Normative EEG microstates and developmental stages. Neuroimage 16:41–48.

Kondakor I, Pascual-Marqui RD, Michel CM, Lehmann D (1995): Event-related potential map differences depend on the prestimulus microstates. J Med Eng Technol 19:66–69.

Kondakor I, Lehmann D, Michel CM, Brandeis D, Kochi K, Koenig T (1997): Prestimulus EEG microstates influence visual event-related potential microstates in field maps with 47 channels. J Neural Transm V104:161–173.

Kornmeier J, Bach M (2004): Early neural activity in Necker-cube reversal: Evidence for low-level processing of a gestalt phenomenon. Psychophysiology 41:1–8.

Kornmeier J, Bach M (2005): The Necker cube—An ambiguous figure disambiguated in early visual processing. Vision Res 45:955–960.

Kornmeier J, Bach M (2006): Bistable perception—Along the processing chain from ambiguous visual input to a stable percept. Int J Psychophysiol 62:345–349.

Kornmeier J, Ehm W, Bigalke H, Bach M (2007): Discontinuous presentation of ambiguous figures: How interstimulus-interval durations affect reversal dynamics and ERPs. Psychophysiology 44:552–560.

Laganaro M, Morand S, Michel CM, Spinelli L, Schnider A: ERP correlates of word production before and after stroke in an aphasic patient. J Cognit Neurosci, in press.

Lee SH, Blake R, Heeger DJ (2005): Traveling waves of activity in primary visual cortex during binocular rivalry. Nat Neurosci 8:22–23.

Lehky S (1995): Binocular rivalry is not chaotic. Proc R Soc Lond Ser B: Biol Sci 259:71–76.

Lehmann D, Ozaki H, Pal I (1987): EEG alpha map series: Brain micro-states by space-oriented adaptive segmentation. Electroencephalogr Clin Neurophysiol 67:271–288.

Lehmann D, Wackermann J, Michel CM, Koenig T (1993): Space-oriented EEG segmentation reveals changes in brain electric field maps under the influence of a nootropic drug. Psychiatry Res 50:275–282.

Lehmann D, Michel CM, Pal I, Pascual-Marqui RD (1994): Event-related potential maps depend on prestimulus brain electric microstate map. Int J Neurosci 74:239–248.

Lehmann D, Strik WK, Henggeler B, Koenig T, Koukkou M (1998): Brain electric microstates and momentary conscious mind states as building blocks of spontaneous thinking: I. Visual imagery and abstract thoughts. Int J Psychophysiol 29:1–11.

Lehmann D, Pascual-Marqui RD, Michel CM (2009): EEG microstates. Scholarpedia 4:7632.

Lehmann D, Pascual-Marqui RD, Strik WK, Koenig T (2010): Core networks for visual-concrete and abstract thought content: A brain electric microstate analysis. Neuroimage 49:1073–1079.

Lehmann D, Skrandies W (1980): Reference-free identification of components of checkerboard-evoked multichannel potential fields. Electroencephalogr Clin Neurophysiol 48:609–621.

Leopold DA, Logothetis NK (1996): Activity changes in early visual cortex reflect monkeys' percepts during binocular rivalry. Nature 379:549–553.

Leopold DA, Logothetis NK (1999): Multistable phenomena: Changing views in perception. Trends Cogn Sci 3:254–264.

Leopold DA, Wilke M, Maier A, Logothetis NK (2002): Stable perception of visually ambiguous patterns. Nat Neurosci 5:605–609.

Logothetis NK, Leopold DA, Sheinberg DL (1996): What is rivalling during binocular rivalry? Nature 380:621–624.

Logothetis NK, Schall JD (1989): Neuronal correlates of subjective visual perception. Science 245:761–763.

Lumer ED, Friston KJ, Rees G (1998): Neural correlates of perceptual rivalry in the human brain. Science 280:1930–1934.

Lumer ED, Rees G (1999): Covariation of activity in visual and prefrontal cortex associated with subjective visual perception. Proc Natl Acad Sci USA 96:1669–1673.

Mamassian P, Goutcher R (2005): Temporal dynamics in bistable perception. J Vis 5:361–375.

Meng M, Remus DA, Tong F (2005): Filling-in of visual phantoms in the human brain. Nat Neurosci 8:1248–1254.

Meng M, Tong F (2004): Can attention selectively bias bistable perception? Differences between binocular rivalry and ambiguous figures. J Vis 4:539–551.

Michel CM, Murray MM, Lantz G, Gonzalez S, Spinelli L, Grave de Peralta R (2004): EEG source imaging. Clin Neurophysiol 115:2195–2222.

Michel CM, Koenig T, Brandeis D, Gianotti L, Wackermann J (2009): Electrical Neuroimaging. Cambridge: Cambridge University Press.

Mohr C, Michel CM, Lantz G, Ortigue S, Viaud-Delmon I, Landis T (2005): Brain state-dependent functional hemispheric specialization in men but not in women. Cereb Cortex 15:1451–1458.

Murray MM, Camen C, Gonzalez Andino SL, Bovet P, Clarke S (2006): Rapid brain discrimination of sounds of objects. J Neurosci 26:1293–1302.

Murray MM, Brunet D, Michel CM (2008): Topographic ERP analyses: A step-by-step tutorial review. Brain Topogr 20:249–264.

Pascual-Marqui RD, Michel CM, Lehmann D (1995): Segmentation of brain electrical activity into microstates: Model estimation and validation. IEEE Trans Biomed Eng 42:658–665.

Pessoa L, Ungerleider LG (2004): Neural correlates of change detection and change blindness in a working memory task. Cereb Cortex 14:511–520.

Phillips C, Mattout J, Rugg MD, Maquet P, Friston KJ (2005): An empirical Bayesian solution to the source reconstruction problem in EEG. Neuroimage 24:997–1011.

Pitts MA, Martinez A, Stalmaster C, Nerger JL, Hillyard SA (2009): Neural generators of ERPs linked with Necker cube reversals. Psychophysiology 46:694–702.

Polonsky A, Blake R, Braun J, Heeger DJ (2000): Neuronal activity in human primary visual cortex correlates with perception during binocular rivalry. Nat Neurosci 3:1153–1159.

Schulz E, Maurer U, van der Mark S, Bucher K, Brem S, Martin E, Brandeis D (2008): Impaired semantic processing during sentence reading in children with dyslexia: Combined fMRI and ERP evidence. Neuroimage 41:153–168.

Sheinberg DL, Logothetis NK (1997): The role of temporal cortical areas in perceptual organization. Proc Natl Acad Sci 94: 3408–3413.

Sidak Z (1967): Rectangular confidence region for the means of multivariate normal distributions. J Am Stat Assoc 62:626–633.

Slotnick SD, Yantis S (2005): Common neural substrates for the control and effects of visual attention and perceptual bistability. Cogn Brain Res 24:97–108.

Sperli F, Spinelli L, Seeck M, Kurian M, Michel CM, Lantz G (2006): EEG source imaging in pediatric epilepsy surgery: A new perspective in presurgical workup. Epilepsia 47:981–990.

Spinelli L, Gonzalez Andino S, Lantz G, Seeck M, Michel CM (2000): Electromagnetic inverse solutions in anatomically constrained spherical head models. Brain Topogr 13:115–125.

Sterzer P, Kleinschmidt A (2007): A neural basis for inference in perceptual ambiguity. Proc Natl Acad Sci USA 104:323–328.

Sterzer P, Kleinschmidt A, Rees G (2009): The neural bases of multistable perception. Trends Cogn Sci 13:310–318.

Sterzer P, Rees G (2008): A neural basis for percept stabilization in binocular rivalry. J Cognit Neurosci 20:389–399.

Tong F, Nakayama K, Vaughan JT, Kanwisher N (1998): Binocular rivalry and visual awareness in human extrastriate cortex. Neuron 21:753–759.

van Dam LCJ, van Ee R (2006): Retinal image shifts, but not eye movements per se, cause alternations in awareness during binocular rivalry. J Vis 6:1172–1179.

VanRullen R, Pascual-Leone A, Battelli L (2008): The continuous Wagon wheel illusion and the "When" pathway of the right parietal lobe: A repetitive transcranial magnetic stimulation study. PLoS ONE 3:e2911.

Vaughan HGJ (1982): The neural origins of human event-related potentials. Ann N Y Acad Sci 388:125–138.

Vulliemoz S, Thornton R, Rodionov R, Carmichael DW, Guye M, Lhatoo S, McEvoy AW, Spinelli L, Michel CM, Duncan JS (2009): The spatio-temporal mapping of epileptic networks: Combination of EEG-fMRI and EEG source imaging. Neuroimage 46:834–843.

Wilcke JC, O'Shea RP, Watts R (2009): Frontoparietal activity and its structural connectivity in binocular rivalry. Brain Res 1305:96–107.

Windmann S, Wehrmann M, Calabrese P, Güntürkün O (2006): Role of the prefrontal cortex in attentional control over bistable vision. J Cognit Neurosci 18:456–471.

Wolfe JM (1983): Influence of spatial frequency, luminance, and duration on binocular rivalry and abnormal fusion of briefly presented dichoptic stimuli. Perception 12:447–456.

Wunderlich K, Schneider KA, Kastner S (2005): Neural correlates of binocular rivalry in the human lateral geniculate nucleus. Nat Neurosci 8:1595–1602.

Zumsteg D, Friedman A, Wieser HG, Wennberg RA (2006): Propagation of interictal discharges in temporal lobe epilepsy: Correlation of spatiotemporal mapping with intracranial foramen ovale electrode recordings. Clin Neurophysiol 117:2615–2626.